Intracellular organisation and tissue interactions underlying lumen formation

Clare E Buckley[1], Xiaoyun Ren[1], Laura C Ward[1], Gemma C Girdler[1], Claudio Araya[1], Mary J Green[1], Brian S Clark[2], Brian A Link[2], Jon D W Clarke[1†]

Running title: Lumen formation *in vivo*

Character count: 56,106

1. MRC Centre for Developmental Neurobiology
King's College London
New Hunt's House, 4th Floor
Guy's Hospital Campus
London SE1 1UL, UK

2. Department of Cell Biology, Neurobiology & Anatomy
Medical College of Wisconsin
8701 Watertown Plank Road
Milwaukee, WI 53226-0509, USA

† Corresponding author: +44 (0)2078486463 jon.clarke@kcl.ac.uk

Abstract

By analysing the cellular and subcellular events that occur in the centre of the developing zebrafish neural rod, we have uncovered a novel mechanism of cell polarisation during lumen formation. Cells from each side of the neural rod interdigitate across the tissue midline. This is necessary for localisation of apical junctional proteins to the region where cells intersect the tissue midline. Cells assemble a mirror-symmetric microtubule cytoskeleton around the tissue midline, which is necessary for the trafficking of proteins required for normal lumen formation, such as Pard3 and Rab11a to this point. This occurs in advance and is independent of the midline cell division that has been shown to have a powerful role in lumen organisation. To our knowledge, this is the first example of the initiation of apical polarisation part way along the length of a cell, rather than at a cell extremity. Although the midline division is not necessary for apical polarisation, it confers a morphogenetic advantage by efficiently eliminating cellular processes that would otherwise bridge the developing lumen.

Key words: apical polarisation/lumen formation/Pard3/Rab11a/zebrafish

Introduction

Generation of epithelial tubes is a common requirement in many embryonic organs. These tubular structures can be different in complexity and function, but they all contain a single central lumen lined by apical membrane connected by cell-cell junctions. The position of the central lumen is mediated by the proper polarisation of the surrounding epithelial cells, which is crucial to lumen function. There are a myriad of human disorders characterised by defects in epithelial cell polarity such as polycystic kidney disease, cystic fibrosis and cancer (Mellman & Nelson, 2008; Wilson, 2011; Wodarz & Nathke, 2007). Understanding the cellular and molecular regulation of cell polarisation and lumen formation and how this is coordinated with whole tissue morphogenesis is therefore key, not only to further our understanding of normal development, but also to determine what goes wrong in these diseases as well as to begin the possibility for engineering epithelial tubes outside the body with a view to tissue replacement and repair.

Although several of the molecular components required for lumen formation have been identified using cells lines in 3-dimensional cultures (Desclozeaux et al, 2008; Jaffe et al, 2008; Rodriguez-Fraticelli et al, 2010), these systems lack the environmental and morphogenetic complexity of the *in vivo* situation. We study lumen formation in the context of whole tissue morphogenesis using *in vivo* live imaging during neurulation in the transparent zebrafish embryo. During this process, neural progenitor (NP) cells first form a solid rod primordium in which cells from the left and right sides transiently interdigitate across the tissue midline (Hong et al, 2010). Cells then establish apical polarity at the tissue midline and subsequently the tissue cavitates to open a lumen at the tissue centre (Clarke, 2009; Kunz, 2004; Lowery & Sive, 2004). We and others previously identified a novel and dominant influence of oriented cell divisions in establishing the position and organization of the developing lumen (Ciruna et al, 2006; Quesada-Hernandez et al, 2010; Tawk et al, 2007; Zigman et al, 2011). These C-divisions (for midline crossing divisions) occur close to the organ centre and generate mirror-symmetric daughters on either side of the nascent lumen. During the C-division a GFP fusion for the polarity protein Partitioning defective 3 (Pard3-GFP) is localised to the cleavage furrow between daughters. This results in the mirror-symmetric distribution of this protein to the region where daughters remain in

contact at the midline (Tawk et al, 2007). This observation suggested that the division itself could be responsible for localizing Pard3-GFP and related polarity proteins to the tissue midline. However several papers have also shown that neural rods in which the midline division is inhibited can still polarise at the midline (Ciruna et al, 2006; Quesada-Hernandez et al, 2010; Tawk et al, 2007; Zigman et al, 2011). Thus other factors must contribute to the establishment of midline polarity and the morphogenetic role of the C-division remains unclear.

Here we uncover a division-independent mechanism that organises cell polarisation at the tissue midline. Apical polarity is established at the point where cells intersect the midline and depends on a mirror-symmetric microtubule cytoskeleton and cell-cell interactions across the midline. We also show that although the C-division is dispensable for midline polarisation, it confers a morphogenetic advantage to the cell remodelling required for lumen formation over non-dividing cells.

Results

Apical polarisation of cells at the tissue midline begins prior to the C-division

We analysed the C-division and the initiation of Pard3-GFP localisation at higher spatial and temporal resolution than previously (Tawk et al, 2007). Most cells interdigitate across the midline prior to the C-division and we find that small puncta of Pard3-GFP first appear broadly localized to the region where cells overlap at the midline (Figure 1A) in advance of the C-division. This suggests that cells recognise the tissue midline prior to division.

The broad localisation of Pard3-GFP puncta around the midline is maintained through metaphase and early telophase as cells undergo mitosis. However cells do not all lie precisely at the midline during cytokinesis (Figure 1B) and this results in some variability in Pard3-GFP distribution during cleavage. Cells dividing exactly at the tissue centre localise Pard3-GFP across the middle of the dividing cell and it accumulates in the cleavage furrow from early stages of telophase (Figure 1C). However, cells whose metaphase plate is lateral to the

midline have an asymmetric location of Pard3-GFP towards their medial side that does not accumulate evenly across the cleavage furrow (Figure 1D). Despite this, even in cells in which Pard3-GFP is initially asymmetrically localised, Pard3-GFP always accumulates on either side of the cleavage plane at later stages of division, as previously reported (Figure 1A, Movie S1) (Tawk et al, 2007). These results show that Pard3-GFP localisation is initiated prior to the C-division and its subcellular distribution through cytokinesis is related to cell position relative to the midline.

Apical polarisation of cells at the tissue midline is independent of cell division

To better understand the division independent mechanisms of cell polarisation, we blocked C-divisions between 9 and 22 hours post fertilisation (h.p.f.) (Figure S1). We found that most cells in the division-blocked neural rod extended across the midline and 43% cells spanned the whole width of the neural rod from left to right hand side (Figure 2A). Blocking cell division thus exaggerated the extent of cell interdigitation across the tissue midline and allowed us to observe the generation of polarity within cells more easily than in wild type embryos. Remarkably, Pard3-GFP puncta were first localized around the point where the cell intersected the tissue midline, irrespective of whether cells spanned the whole width of the rod, or only part of it (Figure 2B, C and D, Movie S2). Immunostaining revealed that the apical tight junction marker zonula occludens 1 (ZO1) was also localised to the region where cells intersected the tissue midline (Figure 2E). Division-blocked cells that spanned the midline initially showed no morphological specialisations at the midline. However, we later observed a dynamic and complex rearrangement of microtubules between the main cell body and the contralateral process (Figure 2F) as they built the apical end-foot that will form part of the lumen surface. In addition, in many cells the contralateral process narrows and retracts back towards the neural midline (Figure 2F).

These results confirm that localization of Pard3-GFP protein at the organ midline is independent of cell division and occurs despite cell extension across the midline. Furthermore cell morphology can be remodelled at the midline to form an apical surface in a division-independent manner.

A mirror-symmetric microtubule cytoskeleton is organised around the tissue midline

Apical protein localisation and cytoskeletal rearrangement around the point where division-blocked cells intersect the midline rather than at the cell's extremity suggests that the machinery of cell polarity may be organised around this point. Since centrosomes are characteristically found at the apical pole of neuroepithelial cells (Taverna & Huttner, 2010) and it has previously been suggested that centrosomes gradually locate to the rod midline during the transition from keel to rod (Hong et al, 2010). We have used live imaging to determine whether this centrosomal location is dependent on cell division. We analysed wild type cells before division, while they still interdigitate across the centre of the tissue. We find that, prior to division, centrosomes gradually locate to whichever part of the cell lies over the tissue midline, despite the main body of the cell often remaining laterally located (Figure 3A). This centrosomal location corresponds broadly with the location of Pard3-GFP puncta seen in cell processes that interdigitate across the midline prior to C-division (Figure 1). Before the cells enter mitosis the nucleus then also moves towards the midline, the duplicated centrosomes separate and the spindle for division is assembled close to the midline (Figure 3A). This suggests that the localisation of centrosomes to the midline is independent of cell division and may be instrumental in specifying the correct location for the C-division. To confirm centrosome location is independent of cell division we analysed this in division-blocked cells and also found that centrosomes were located very close to where these cells intersected the midline, rather than at the cells' extremity (Figure 3B).

The location of centrosomes part-way along the cell suggested that microtubule polarity might be organised around this point. To test this, we analysed expression of End binding protein 3-GFP (EB3-GFP), a marker of the plus-ends of growing microtubules (Stepanova et al, 2003) in division-blocked cells. EB3-GFP microtubule tips were found to grow mirror-symmetrically away from the microtubule organising centre (MTOC), close to where each cell intersected the tissue midline (Figure 3Ci and ii and Movie S3). Microtubule polarity is thus reversed around the point at which division blocked cells intersect the midline.

We also observed the same mirror-reversal of microtubule polarity in wild-type cells that protrude across the neural rod midline before C-division (Figure 3Di and ii, Movie S4). The spindle for division is then assembled close to the midline and, following C-division, the MTOCs are gradually repositioned towards the midline, where the daughters remain attached to each other (Tawk et al, 2007) (Figure 3Diii).

These results demonstrate that mirror-symmetric microtubule polarity within individual cells is organised around the neural rod midline prior to and independent of C-division, and suggest that microtubule dependent processes could underlie the delivery of proteins required for lumen formation to the apical midline.

Pard3 fusion proteins are mis-localised following nocodazole treatment

In order to test whether apical polarisation at the neural rod midline is dependent on microtubule-mediated transport, we depolymerised microtubules in division-blocked embryos using nocodazole treatment. In untreated embryos Pard3 fusion protein begins to accumulate at the neural midline in some cells in the early neural keel and is localised to the middle of the rod in all cells by 17-19 somite stages (Figure 2B-D). Following addition of 5ug/mL nocodazole at the 7-somite stage many cells expressed Pard3 fusion protein at the neural rod midline shortly after treatment (Figure 4Bi, 7 somites). However, by the equivalent of the 10-somite stage, 88% cells in treated embryos had localised some (Figure 4Bi) or all (Figure 4Bii) Pard3 fusion protein ectopically to their basal side (Figure 4C). At this stage microtubules had been extensively depolymerised (Figure 4A). However, cells were able to recover after nocodazole wash out: Par3-GFP puncta gradually moved from the basal to apical sides of cells, along microtubule-like structures (Figure 4Dii arrows) and the Pard3-GFP domain was re-established at the apical side of cells (Figure 4D). A previous study (Hong et al, 2010) has suggested that Pard3 polarisation is independent of microtubules, but we suggest that their shorter nocodazole treatment may be insufficient to reveal the importance of microtubules. Our results demonstrate that apical localisation of Pard3 is dependent on microtubule-mediated transport, apparently with a plus to minus end directionality. This suggests that the intracellular reversal of

microtubule polarity around the midline is a key step in establishing the correct localisation of apical proteins.

Pard3 and Rab11a are necessary for lumen formation

In order to test the importance of microtubule-mediated protein transport in lumen formation, we first expressed a mutant form of Pard3, Pard3-Δ6-EGFP, which lacks amino acids 688-1127, including the aPKC-binding domain. This results in binding to microtubules and a lack of specific apical localisation (Tawk et al, 2007; von Trotha et al, 2006). Embryos expressing Pard3-Δ6-EGFP had severely disrupted ventricle morphology in comparison to wild-types (Figure 5A and B), demonstrating that Pard3 function is necessary for normal lumen formation.

Next, we considered the small GTPase Rab Protein 11a (Rab11a). Previous work has suggested that Rab11a is required for apically directed traffic and lumen formation in MDCK cell cysts and Drosophila embryos (Bryant et al, 2010; Desclozeaux et al, 2008; Lock & Stow, 2005; Roeth et al, 2009; Schluter et al, 2009). Furthermore, apical traffic of Rab11a positive endosomes in vitro is dependent on microtubules (Schluter et al, 2009; Xu et al, 2011) and it has been suggested that Rab11a endosomes are necessary to target Pard3 to the apical domain (Bryant et al, 2010). To determine whether Rab11a has a role in lumen formation in zebrafish, we expressed dominant negative Rab11a (Rab11a S25N, abbreviated to Rab11aDN) specifically in all cells in rhombomeres 3 and 5 from approximately the 6-somite stage. This resulted in a complete loss of lumen formation in rhombomeres 3 and 5 (Figure 5C to H. Since Rab11 is known to be required for abscission (Fielding et al, 2005; Pohl & Jentsch, 2008; Skop et al, 2001; Wilson et al, 2005; Yu et al, 2007), the loss of lumen opening could result from a lack of abscission between sister cells at the midline. However, when we blocked cell division in these embryos, lumen opening remained absent in Rab11aDN rhombomeres but was present in adjacent rhombomeres (Figure 5I). Thus lumen opening is independent of cell division and loss of Rab11a function must prevent lumen opening by inhibiting other processes.

To determine the role of Rab11a in the delivery of proteins to the apical domain and in junctional organisation, we analysed the expression of Pard3-GFP, ZO-1,

aPKC and Crb2a in Rab11aDN rhombomeres and of Pard3-RFP in RAB11ADN-EGFP cells. Surprisingly, Pard3-RFP is localised normally to the apical end feet of Rab11aDN-EGFP cells (Figure 5J) and the localisation of all these proteins to the neural midline was initially normal in rhombomeres 3 and 5 at late rod stages. However, their distribution within the plane of the midline was slightly less homogenous than in controls and the level of Crb2a staining was reduced compared to controls (Figure 5F and G and Figure S2). At later stages, when the lumen is just about to open, the relative protein expression levels of aPKC are further reduced and the distribution of proteins along the midline plane becomes irregular and characterised by clumps of immunoreactivity separated by distinct stain-free zones (Figure S2), reminiscent of the mislocalised crumbs localisation seen in the zebrafish hindbrain previously (Clark et al, 2011). By 31 h.p.f., apical proteins were increasingly disorganised and no longer confined to the midline in Rab11aDN rhombomeres (Figure 5L). Together, this data suggests that Rab11a is required for the maintenance of the coherent planar organisation of apical protein complexes at the tissue midline, and that this disruption to junctional organisation inhibits lumen opening.

RAB11A traffic progressively localises to the tissue midline and is mislocalised following nocodazole treatment

Having established the importance of Rab11a as a key player in lumen assembly, we investigated whether Rab11a traffic is also directed to the point where cells intersect the tissue midline. In wild type cells, RAB11A-EGFP endosomes were initially broadly localized around the region where cells intersected the midline. As cells entered mitosis their nuclei moved to the RAB11A-EGFP domain and, following division, the RAB11A-EGFP endosomes became redistributed around the apical pole of each sister cell (Figure 6A, Movie S5). We next analysed RAB11A-EGFP localisation in division-blocked cells. At early neural rod stages, RAB11A-EGFP vesicles were similarly broadly localised around the region where cells intersected the midline. The distribution of RAB11A-EGFP vesicles became increasingly restricted over time until, at late neural rod stages, a precise focus of RAB11A-EGFP vesicles was formed near the midline of the neural rod (Figure 6B, Movie S6). This restriction of RAB11A-EGFP vesicles coincided temporally and spatially with the rearrangement of microtubules where they intersected the

midline (Figure 6B arrow and see figure 2F). In line with previous literature (Schluter et al, 2009), we found RAB11A trafficking to be microtubule dependent, since treatment with nocodazole resulted in the ectopic localisation of RAB11A-EGFP to the basal end of cells, supporting recent *in vitro* results (Xu et al, 2011) (Figure 6C). Together these results demonstrate that RAB11A positive endosomes carry cargo necessary for lumen formation and are targeted to the point at which the cells intersect the tissue midline by a microtubule dependent mechanism. This process is independent of cell division.

Cells integrate anti-basal signals with cell-cell interactions to determine localisation of apical complexes

The assembly of apical complexes around the point where cells intersect the midline could be determined by a cell autonomous mechanism that somehow measures where in the cell these complexes should be positioned. Alternatively interactions between cells that meet at the midline could determine the position of apical complex assembly. To test the latter hypothesis we prevented interactions between cells from the left and right sides by physically dividing the neural plate along the midline using tungsten knives. This physical intervention slows the convergence of cells to the midline and often prevents them meeting their contralateral counterparts. In these circumstances wild-type cells undergo ectopic C-divisions and generate ectopic lumens (Tawk et al, 2007). However when division was blocked, cells assembled apical complexes at the most superficial surface of the neural tissue rather than at some point along the cell length (Figure 7A). This indicates that, in the absence of interactions with contralateral cells, neural cells have an underlying propensity to assemble apical complexes at their most anti-basal extremity.

If interactions with contralateral cells do organise the distribution of apical complexes, then markers of cell-cell junctions should coincide spatially with zones of left-right interdigitation in the neural keel and rod. To test this we analysed nascent cadherin-based cell-cell interactions using Gt(Ctnna-citrine)ct3a transgenic embryos (Zigman et al, 2011) in which we blocked division. During neural keel stages, ctnna-citrine puncta were present along the cells' lateral membrane rather than confined to the cells' anti-basal extremity

(Figure 7Bi). Ctnna-citrine puncta were accurately localised within the zone of cell interdigitation across the tissue midline (Figure 7Biv). This supports the view that a zone of left-right interactions defines the initial localisation of cell-cell junctions and can counteract the default anti-basal localisation of apical complexes.

We hypothesised that extra-cellular matrix (ECM) interactions with the basal ends of cells might be responsible for mediating the underlying anti-basal polarisation of NP cells since ECM has recently been implicated in specifying intercellular junctional position (Tseng et al, 2012) as well as centrosome position and lumen formation (Rodriguez-Fraticelli et al, 2012). To test this we knocked down Laminin C1 using a morpholino (Parsons et al, 2002) to disrupt Laminin 1 incorporation into the basement membrane. In support of *in vitro* data (Myllymaki et al, 2011; O'Brien et al, 2001; Yu et al, 2005), this resulted in the ectopic basal accumulation of normally apically localised GFP-ZO1 in the hindbrain (Figure 7C). This suggests that ECM components are at least partially responsible for the underlying anti-basal localisation of apical complexes.

Lumen surface is disrupted without division

Our observations of apical polarisation within the middle of division-blocked cells demonstrate that cells can build apical specialisations close to the centre of the neural rod independently of the C-division, therefore suggesting that the role of C-division is not to confer appropriate apico-basal polarity to neuroepithelial cells. Although not necessary to organise cell polarity in the neural rod, the C-division may none the less confer a morphological advantage to lumen formation. Therefore we analysed the structure of lumens built with and without the C-division. Whilst the nascent lumen in 18 h.p.f. control embryos was outlined by two continuous ZO1 domains at the hindbrain midline, in division-blocked embryos the domains of ZO1 immunoreactivity were interrupted by cell nuclei that remained straddling the midline (Figure 8A and B). This cell bridging phenotype was especially prevalent at rhombomere boundaries in the hindbrain. However, analysis at spinal cord levels also revealed discontinuous ZO1 domains, thus demonstrating that this phenotype is not unique to rhombomere boundaries. By 22 h.p.f., lumen opening was disorganised and the forming lumen surface was ragged in division-blocked embryos compared to wild-types (Figure

8C). The lumen was still not fully inflated by 24h.p.f. and ventricle opening was particularly restricted at rhombomere boundaries (Figure 8C, arrows), coinciding with the highest prevalence of cell bridges seen at 18h.p.f.. Analysis of individual division-blocked cells demonstrated that in 58% of cells the contralateral process became very narrow and then retracted back to the midline by 16.5hpf (Figure 8D), while the remaining 42% of cells bridging the midline failed to retract their contralateral process by the end of our time-lapse analyses at approximately 19hpf, and remained straddling the midline. By contrast, at this time in wild type embryos, C-division has finished and we have not observed any remaining cell processes that span the midline. Thus although cells can resolve interdigitation across the midline in the absence of the C-division, this process is less efficient. These results demonstrate that the C-division is not required for lumen formation but helps to remove nuclei and cell processes that would otherwise remain bridging the tissue midline and disrupt lumen opening.

Discussion

A novel mechanism of lumen formation at the tissue midline

In tissues that generate a lumen from a solid primordium, two important processes must occur. First, cells must assemble apical membrane and cell-cell junctions at the centre of the organ primordium. Secondly, cells that intersect the organ centre must be removed or remodelled to allow the lumen to open. Our analyses of lumen formation in the zebrafish neural tube reveal several novel cellular and sub-cellular events that underlie these events *in vivo*. A graphical model for our results is depicted in Figure 9. We show that prior to lumen formation, cells in the neural rod are interdigitated across the midline and surprisingly are able to assemble the apical and junctional machinery necessary for lumen formation at the point where they intersect the tissue midline rather than at their extremity. This occurs independently of division. The ability of junctions to relocalise along the length of epithelial cells has been demonstrated recently (Wang et al, 2012) but to our knowledge this is the first example of the initiation of apical polarisation part way along the length of a cell, rather than at a cell extremity. We propose that this novel process of cell polarisation occurs via the following mechanism:

First, we show that NP cells have an underlying propensity to assemble apical complexes at their most anti-basal extremity, which is at least partially mediated by the surrounding ECM at their basal ends. Second, we show that the initial interdigitation of cells at keel stages is necessary to refine this anti-basal polarisation to the area of interdigitation around the tissue midline. We suggest that nascent adhesions form between interdigitating cells from each side of the neural rod and determine the coarse location of apical polarisation to this region within the cells. Third, we suggest that apical protein puncta might then be responsible for centrosome localisation at the midline, which is likely to be upstream of the mirror-symmetric microtubule organisation that we demonstrate occurs around this point. This reinforces and refines the delivery of microtubule-dependent apical proteins such as Pard3 and Rab11a (the function of which we show is necessary for lumen formation) to the midline and an organised planar apical epithelium is formed. This circulatory loop is not dissimilar to that proposed

for the localisation of Par protein domains during cytokinesis of the one-cell stage *C.elegans* embryo (Schenk et al, 2010).

Once the apical epithelium has successfully formed, it is necessary to resolve cell interdigitation across the midline in order to allow efficient lumen opening. In normal embryos this occurs via oriented cytokinesis across the midline (Quesada-Hernandez et al, 2010; Tawk et al, 2007; Zigman et al, 2011), when localisation of the cleavage plane to the tissue midline ensures that cells no longer bridge across the tissue centre. In the absence of cell division we find that cell processes that bridge the tissue midline are retracted back to the point in the cells where they are assembling apical and junctional machinery. However, this process is a less efficient mechanism to clear cellular bridges and nuclei from the midline than the process of division. Therefore, although we demonstrate that the specialised midline division is not necessary for apical domain formation, it does mediate the efficient reorganisation of cells at the midline, and is therefore necessary for organised lumen opening. This work therefore provides further evidence for the importance of regulating cytokinesis during morphogenesis (Baena-Lopez et al, 2005; da Silva & Vincent, 2007; Grosshans & Wieschaus, 2000; Woolner & Papalopulu, 2012).

Although the orientation of junction-mediated polarity differs in different cell types, cadherin and catenin based junctional formation has been shown to be important in mediating the intracellular organisation necessary for cell polarisation in various cell types (Capaldo & Macara, 2007; Chilov et al, 2011; Desai et al, 2009; Dupin et al, 2009; Nejsum & Nelson, 2007; Yang et al, 2009; Zigman et al, 2011), therefore supporting our hypothesis that nascent adhesions between interdigitating cells might initiate apical organisation within the interdigitation zone. The coordination of adhesion with polarity during early junctional maturation has also recently been demonstrated in keratinocytes (Gladden et al, 2010) and nascent cell-cell adhesion clusters between zebrafish NP cells have been shown to be important in defining the division angle of C-divisions (Zigman et al, 2011).

We suggest that the correct localisation of the centrosome at the midline of the tissue is likely to be a key event in reinforcing correct apico-basal polarity. It is known to play a role in initial microtubule organisation of epithelial cells (Bellett et al, 2009) and a recent study in *C. elegans* intestinal epithelia suggests that the centrosome is also necessary to establish later nucleation of microtubules at the apical surface (Feldman & Priess, 2012). We show that centrosome location at the midline precedes nuclear migration to and mitotic spindle formation at the midline. Centrosome localisation could therefore play the dual role of directing apical proteins to the correct location and co-ordinating this with the location of the midline mitoses that play such a powerful role in lumen organisation (Quesada-Hernandez et al, 2010; Tawk et al, 2007; Zigman et al, 2011). Previous work has shown that apical proteins such as Pard3 are necessary for determining centrosome positioning and spindle position in several different cell types (Cai et al, 2003; Feldman & Priess, 2012; Grill et al, 2001; Hong et al, 2010; Kemphues et al, 1988; Schmoranzer et al, 2009) and aPKC has also recently been implicated in centrosomal positioning and subsequent lumen formation in MDCK cells (Rodriguez-Fraticelli et al, 2012). This therefore supports our hypothesis that initial apical protein localisation may drive centrosomal movement to the tissue midline, which then organises the microtubule cytoskeleton around this point and directs the trafficking of Pard3 and Rab11a.

Rab11a is necessary for lumen opening but not for initial midline formation

We demonstrate that functional Rab11a is required for neural lumen opening and the maintenance of a coherent planar organised apical epithelium *in vivo*. Like Pard3, RAB11A-EGFP endosomes are targeted to the point at which the cells intersect the tissue midline via a microtubule-mediated and division-independent mechanism. Therefore, RAB11A trafficking provides another example of a process that is organised around the cells' intersection with the midline in order to assemble a lumen.

Surprisingly, despite the lower levels of Crb2a staining in Rab11aDN rhombomeres at the late rod stage, the initial location of apical proteins is at the midline in all rhombomeres. It is only at later developmental stages that protein staining at the midline significantly decreases, (especially aPKC staining), the

apical epithelium becomes disorganised and the lumen fails to open within Rab11aDN rhombomeres 3 and 5. The early downregulation of Crb2a staining is in line with a study in Drosophila, which shows that a loss of Crb from the cortex of the embryonic ectoderm as a consequence of Rab11DN expression precedes adherens junction destabilisation (Roeth et al, 2009) and supports data suggesting that Rab11a is directly necessary for Crumbs localisation to apical surfaces (Fletcher et al, 2012; Roeth et al, 2009; Schluter et al, 2009). There are many interactions between the Crumbs and Par polarity complexes. For example, loss of Crumbs or of the retromer complex that traffics it in Drosophila embryos prevents the apical localisation of aPKC (Pocha et al, 2011) and a feedback loop between Crumbs and aPKC maintenance at the plasma membrane has also been suggested (Fletcher et al, 2012). Our data therefore suggests that Rab11a is not necessary for the initial polarised delivery of apical junctional components but is necessary for the maintenance of epithelial organisation, at least partly through localising Crumbs proteins to the apical domain.

The lack of lumen opening in Rab11aDN rhombomeres could be downstream of Rab11a's known role in abscission (Fielding et al, 2005; Pohl & Jentsch, 2008; Skop et al, 2001; Wilson et al, 2005; Yu et al, 2007) since a lack of abscission between sister cells bridging the neural midline could explain the lack of lumen opening seen on expression of a dominant negative Rab11a. However, our results suggest that the lack of lumen opening is not inherently related to cytokinesis. It is not clear whether the loss of apical complex proteins that we found in Rab11aDN rhombomeres may mediate the lumen opening phenotype and/or the mislocalisation of junctional proteins later in development. It is possible that there is a separate requirement for Rab11a in resolving junctional disassembly, which is likely necessary for the separation of contralateral cells during lumen opening. Determining the molecular and cellular basis of Rab11a's role in neural tube formation is an important future goal.

Conclusions

Our work advances our understanding of lumen formation *in vivo* by identifying a novel process of cell polarisation, the location of which is determined by cell interdigitation across the tissue midline during convergence. Midline polarisation of proteins necessary for lumen formation, such as Pard3-GFP and RAB11A-EGFP, occurs prior to and independent of the midline division and is dependent on a mirror-symmetric microtubule cytoskeleton. Although division is dispensable for cell polarisation it confers a morphogenetic advantage to cell remodelling and lumen formation over non-dividing cells.

Materials and methods

Blocking cell divisions

To block cell divisions during neurulation, embryos were injected with 0.5-1nl of 0.5mM *emi1* morpholino (*emi1*MO) at a 1 to 4-cell stage. Blocking *emi1* was previously shown to arrest cells in the G2 phase of the cell cycle (Rhodes et al, 2009; Zhang et al, 2008). This efficiently blocked cell division between 9 and 22 h.p.f. (Figure S1). Control embryos were injected with standard control morpholino at the same concentration and stage.

Nocodazole treatment

To break down the microtubule cytoskeleton during neurulation, embryos were treated with 5µg/mL (17µM) nocodazole from 7 somites. This concentration range is above stoichiometric levels (µM range) and causes depolymerisation of microtubules (Gallo & Letourneau, 1999; Jordan & Wilson, 1998). One affect of nocodazole treatment is to arrest dividing cells in prometaphase, resulting in the persistent rounding up of cells. To isolate the effects of nocodazole on polarisation from these complicating effects on division, we also blocked division using *emi1*MO. This allowed most cells to maintain an elongated morphology and the apicobasal location of Pard3 fusion proteins could therefore be assessed within cells that had a disorganised microtubule cytoskeleton. Embryos remained in nocodazole solution for 1 hour and 30 minutes during imaging until the equivalent of the 10-somite stage.

Dextran injection

To enable visualisation of ventricular morphology, a small volume of 4% rhodamine dextran was injected into the hindbrain ventricles of 28 h.p.f. embryos.

Abrogating Rab11a function

We crossed a UAS-inducible dominant-negative Rab11a line of zebrafish Tg(UAS:mCherry-Rab11a S25N)^{mw35} (Clark et al, 2011) with a line of zebrafish in which the optimised Gal4-activator, KalTA4, is driven by Krox20 specifically in rhombomeres 3 and 5 from approximately the 6 somite stage tg(*Krox20-RFP-KalTA4*) (Distel et al, 2009). This resulted in expression of Rab11a-S25N

specifically in rhombomeres 3 and 5. The S25N version of Rab11a does not bind GTP and so is maintained in the GDP form and inhibits recycling.

Preventing convergence

Prior to convergence, at 10 h.p.f., *emi1*MO-injected embryos were mounted in agarose and the neural plate was bisected at the midline using a tungsten needle. Embryos were allowed to heal in E2 embryo medium with penicillin/streptomycin (1%, Invitrogen) for 3 hours, removed from agarose and incubated until the 16-18-somite stage.

Data Analysis

Division position analysis: To measure the position of C-divisions, time-lapse movies of nuclei labelled with H2B-RFP were taken at the level of the hindbrain between the otic vesicles. The midline position was defined as the midpoint between the left and right edges of the neural tube as observed in bright-field. Division position was measured from the midline to the metaphase plate of each division from both horizontal and transverse sections.

Pard3-FP sub-cellular location during nocodazole treatment: Embryos were selected from different experiments; some of which were mosaically labelled with Pard3-GFP and some with Pard3-RFP to ensure that conditions were not bias towards one experiment. Contingency tables were drawn to compare the number of cells containing some basal Pard3-FP with the number containing exclusively apical Pard3-FP or no Pard3-FP in nocodazole-treated and control embryos. This was done for the 6-somite stage (before nocodazole treatment) and at the equivalent of the 10-somite stage (1 hour 30 minutes after nocodazole treatment). These tables were used to carry out Fisher's exact test.

Nascent lumen surface analysis: Tissue bridges across the neural rod midline were visualised by ZO1 immunostaining and a sytox nuclei counter stain. The number of midline bridges was counted along the entire dorsal-ventral axes in a horizontal 150μm region surrounding the otic vesicle for 7 embryos from each

group (*emi* MO vs. control MO). A two-tailed unpaired T-test was used to compare numbers of bridges between each treatment group.

Acknowledgements

We thank Paula Alexandre, Antonino Schepis, Andrew Symonds, Corinne Houart, Phillip Gordon-Weeks and Andrew Lumsden for helpful comments on the manuscript. Also thank you to Gwynn, Bill Harris, Masa Tada, Steve Wilson and Felix Loosli for constructs. Thank you to David Wilkinson for the Krox20-RFP-KalTA4 fish line and to Mihaela Zigman for the Gt(Ctnna-citrine)ct3a line. *This work was funded by the BBSRC, MRC, Wellcome Trust, National Institute of Health and National Eye Institute.*

Author Contributions

Clare Buckley co-wrote the manuscript and produced the work for movies 3-7 and figures 3, 4, 5C-L, 6, 9 and S2. Xiaoyun Ren produced the work for movies 1-2 and figures 2, 8 and S1. Xiaoyun Ren and Gemma Girdler together produced the work for figures 1A-B. Laura Ward produced the work for figures 1C and 7. Claudio Araya produced the work for figure 5A-B. Mary Green contributed to the analysis of division-blocked cells. Brian Clark and Brian Link made the Tg(UAS:mCherry-Rab11a S25N)^{mw35} line of zebrafish. Jon Clarke oversaw the whole project and co-wrote the manuscript.

Conflict of Interest

The authors declare that they have no conflict of interest

References

Baena-Lopez LA, Baonza A, Garcia-Bellido A (2005) The orientation of cell divisions determines the shape of Drosophila organs. *Curr Biol* **15:** 1640-1644

Bellett G, Carter JM, Keynton J, Goldspink D, James C, Moss DK, Mogensen MM (2009) Microtubule plus-end and minus-end capture at adherens junctions is involved in the assembly of apico-basal arrays in polarised epithelial cells. *Cell motility and the cytoskeleton* **66:** 893-908

Bryant DM, Datta A, Rodriguez-Fraticelli AE, Peranen J, Martin-Belmonte F, Mostov KE (2010) A molecular network for de novo generation of the apical surface and lumen. *Nat Cell Biol* **12:** 1035-1045

Cai Y, Yu F, Lin S, Chia W, Yang X (2003) Apical complex genes control mitotic spindle geometry and relative size of daughter cells in Drosophila neuroblast and pI asymmetric divisions. *Cell* **112:** 51-62

Capaldo CT, Macara IG (2007) Depletion of E-cadherin disrupts establishment but not maintenance of cell junctions in Madin-Darby canine kidney epithelial cells. *Mol Biol Cell* **18:** 189-200

Chilov D, Sinjushina N, Rita H, Taketo MM, Makela TP, Partanen J (2011) Phosphorylated beta-catenin localizes to centrosomes of neuronal progenitors and is required for cell polarity and neurogenesis in developing midbrain. *Developmental biology* **357:** 259-268

Ciruna B, Jenny A, Lee D, Mlodzik M, Schier AF (2006) Planar cell polarity signalling couples cell division and morphogenesis during neurulation. *Nature* **439:** 220-224

Clark BS, Winter M, Cohen AR, Link BA (2011) Generation of Rab-based transgenic lines for in vivo studies of endosome biology in zebrafish. *Dev Dyn* **240:** 2452-2465

Clarke J (2009) Role of polarized cell divisions in zebrafish neural tube formation. *Curr Opin Neurobiol* **19:** 134-138

da Silva SM, Vincent JP (2007) Oriented cell divisions in the extending germband of Drosophila. *Development* **134:** 3049-3054

Desai RA, Gao L, Raghavan S, Liu WF, Chen CS (2009) Cell polarity triggered by cell-cell adhesion via E-cadherin. *Journal of cell science* **122:** 905-911

Desclozeaux M, Venturato J, Wylie FG, Kay JG, Joseph SR, Le HT, Stow JL (2008) Active Rab11 and functional recycling endosome are required for E-cadherin trafficking and lumen formation during epithelial morphogenesis. *American journal of physiology Cell physiology* **295:** C545-556

Distel M, Wullimann MF, Koster RW (2009) Optimized Gal4 genetics for permanent gene expression mapping in zebrafish. *Proc Natl Acad Sci U S A* **106:** 13365-13370

Dupin I, Camand E, Etienne-Manneville S (2009) Classical cadherins control nucleus and centrosome position and cell polarity. *The Journal of cell biology* **185:** 779-786

Feldman JL, Priess JR (2012) A role for the centrosome and PAR-3 in the hand-off of MTOC function during epithelial polarization. *Curr Biol* **22:** 575-582

Fielding AB, Schonteich E, Matheson J, Wilson G, Yu X, Hickson GR, Srivastava S, Baldwin SA, Prekeris R, Gould GW (2005) Rab11-FIP3 and FIP4 interact with Arf6 and the exocyst to control membrane traffic in cytokinesis. *EMBO J* **24:** 3389-3399

Fletcher GC, Lucas EP, Brain R, Tournier A, Thompson BJ (2012) Positive feedback and mutual antagonism combine to polarize crumbs in the Drosophila follicle cell epithelium. *Curr Biol* **22:** 1116-1122

Gallo G, Letourneau PC (1999) Different contributions of microtubule dynamics and transport to the growth of axons and collateral sprouts. *J Neurosci* **19:** 3860-3873

Gladden AB, Hebert AM, Schneeberger EE, McClatchey AI (2010) The NF2 tumor suppressor, Merlin, regulates epidermal development through the establishment of a junctional polarity complex. *Developmental cell* **19:** 727-739

Grill SW, Gonczy P, Stelzer EH, Hyman AA (2001) Polarity controls forces governing asymmetric spindle positioning in the Caenorhabditis elegans embryo. *Nature* **409:** 630-633

Grosshans J, Wieschaus E (2000) A genetic link between morphogenesis and cell division during formation of the ventral furrow in Drosophila. *Cell* **101:** 523-531

Hong E, Jayachandran P, Brewster R (2010) The polarity protein Pard3 is required for centrosome positioning during neurulation. *Developmental biology* **341:** 335-345

Jaffe AB, Kaji N, Durgan J, Hall A (2008) Cdc42 controls spindle orientation to position the apical surface during epithelial morphogenesis. *The Journal of cell biology* **183:** 625-633

Jordan MA, Wilson L (1998) Use of drugs to study role of microtubule assembly dynamics in living cells. *Methods Enzymol* **298:** 252-276

Kemphues KJ, Priess JR, Morton DG, Cheng NS (1988) Identification of genes required for cytoplasmic localization in early C. elegans embryos. *Cell* **52:** 311-320

Kunz YW (2004) *Developmental Biology of Teleost Fishes*: Springer.

Lock JG, Stow JL (2005) Rab11 in recycling endosomes regulates the sorting and basolateral transport of E-cadherin. *Mol Biol Cell* **16:** 1744-1755

Lowery LA, Sive H (2004) Strategies of vertebrate neurulation and a re-evaluation of teleost neural tube formation. *Mech Dev* **121:** 1189-1197

Mellman I, Nelson WJ (2008) Coordinated protein sorting, targeting and distribution in polarized cells. *Nat Rev Mol Cell Biol* **9:** 833-845

Myllymaki SM, Teravainen TP, Manninen A (2011) Two distinct integrin-mediated mechanisms contribute to apical lumen formation in epithelial cells. *PloS one* **6:** e19453

Nejsum LN, Nelson WJ (2007) A molecular mechanism directly linking E-cadherin adhesion to initiation of epithelial cell surface polarity. *The Journal of cell biology* **178:** 323-335

O'Brien LE, Jou TS, Pollack AL, Zhang Q, Hansen SH, Yurchenco P, Mostov KE (2001) Rac1 orientates epithelial apical polarity through effects on basolateral laminin assembly. *Nat Cell Biol* **3:** 831-838

Parsons MJ, Pollard SM, Saude L, Feldman B, Coutinho P, Hirst EM, Stemple DL (2002) Zebrafish mutants identify an essential role for laminins in notochord formation. *Development* **129:** 3137-3146

Pocha SM, Wassmer T, Niehage C, Hoflack B, Knust E (2011) Retromer controls epithelial cell polarity by trafficking the apical determinant Crumbs. *Curr Biol* **21:** 1111-1117

Pohl C, Jentsch S (2008) Final stages of cytokinesis and midbody ring formation are controlled by BRUCE. *Cell* **132:** 832-845

Quesada-Hernandez E, Caneparo L, Schneider S, Winkler S, Liebling M, Fraser SE, Heisenberg CP (2010) Stereotypical Cell Division Orientation Controls Neural Rod Midline Formation in Zebrafish. *Curr Biol*

Rhodes J, Amsterdam A, Sanda T, Moreau LA, McKenna K, Heinrichs S, Ganem NJ, Ho KW, Neuberg DS, Johnston A, Ahn Y, Kutok JL, Hromas R, Wray J, Lee C, Murphy C, Radtke I, Downing JR, Fleming MD, MacConaill LE, Amatruda JF, Gutierrez A, Galinsky I, Stone RM, Ross EA, Pellman DS, Kanki JP, Look AT (2009) Emi1 maintains genomic integrity during zebrafish embryogenesis and cooperates with p53 in tumor suppression. *Molecular and cellular biology* **29:** 5911-5922

Rodriguez-Fraticelli AE, Auzan M, Alonso MA, Bornens M, Martin-Belmonte F (2012) Cell confinement controls centrosome positioning and lumen initiation during epithelial morphogenesis. *The Journal of cell biology* **198:** 1011-1023

Rodriguez-Fraticelli AE, Vergarajauregui S, Eastburn DJ, Datta A, Alonso MA, Mostov K, Martin-Belmonte F (2010) The Cdc42 GEF Intersectin 2 controls mitotic spindle orientation to form the lumen during epithelial morphogenesis. *The Journal of cell biology* **189:** 725-738

Roeth JF, Sawyer JK, Wilner DA, Peifer M (2009) Rab11 helps maintain apical crumbs and adherens junctions in the Drosophila embryonic ectoderm. *PloS one* **4:** e7634

Schenk C, Bringmann H, Hyman AA, Cowan CR (2010) Cortical domain correction repositions the polarity boundary to match the cytokinesis furrow in C. elegans embryos. *Development* **137:** 1743-1753

Schluter MA, Pfarr CS, Pieczynski J, Whiteman EL, Hurd TW, Fan S, Liu CJ, Margolis B (2009) Trafficking of Crumbs3 during cytokinesis is crucial for lumen formation. *Mol Biol Cell* **20:** 4652-4663

Schmoranzer J, Fawcett JP, Segura M, Tan S, Vallee RB, Pawson T, Gundersen GG (2009) Par3 and dynein associate to regulate local microtubule dynamics and centrosome orientation during migration. *Curr Biol* **19:** 1065-1074

Skop AR, Bergmann D, Mohler WA, White JG (2001) Completion of cytokinesis in C. elegans requires a brefeldin A-sensitive membrane accumulation at the cleavage furrow apex. *Curr Biol* **11:** 735-746

Stepanova T, Slemmer J, Hoogenraad CC, Lansbergen G, Dortland B, De Zeeuw CI, Grosveld F, van Cappellen G, Akhmanova A, Galjart N (2003) Visualization of microtubule growth in cultured neurons via the use of EB3-GFP (end-binding protein 3-green fluorescent protein). *J Neurosci* **23:** 2655-2664

Taverna E, Huttner WB (2010) Neural progenitor nuclei IN motion. *Neuron* **67:** 906-914

Tawk M, Araya C, Lyons DA, Reugels AM, Girdler GC, Bayley PR, Hyde DR, Tada M, Clarke JD (2007) A mirror-symmetric cell division that orchestrates neuroepithelial morphogenesis. *Nature* **446:** 797-800

Tseng Q, Duchemin-Pelletier E, Deshiere A, Balland M, Guillou H, Filhol O, Thery M (2012) Spatial organization of the extracellular matrix regulates cell-cell junction positioning. *Proc Natl Acad Sci U S A* **109:** 1506-1511

von Trotha JW, Campos-Ortega JA, Reugels AM (2006) Apical localization of ASIP/PAR-3:EGFP in zebrafish neuroepithelial cells involves the oligomerization domain CR1, the PDZ domains, and the C-terminal portion of the protein. *Dev Dyn* **235:** 967-977

Wang YC, Khan Z, Kaschube M, Wieschaus EF (2012) Differential positioning of adherens junctions is associated with initiation of epithelial folding. *Nature*

Wilson GM, Fielding AB, Simon GC, Yu X, Andrews PD, Hames RS, Frey AM, Peden AA, Gould GW, Prekeris R (2005) The FIP3-Rab11 protein complex regulates recycling endosome targeting to the cleavage furrow during late cytokinesis. *Mol Biol Cell* **16:** 849-860

Wilson PD (2011) Molecular mechanisms of polycystic kidney disease. *Biochimica et biophysica acta* **1812:** 1201

Wodarz A, Nathke I (2007) Cell polarity in development and cancer. *Nat Cell Biol* **9:** 1016-1024

Woolner S, Papalopulu N (2012) Spindle position in symmetric cell divisions during epiboly is controlled by opposing and dynamic apicobasal forces. *Developmental cell* **22:** 775-787

Xu S, Edman M, Kothawala MS, Sun G, Chiang L, Mircheff A, Zhu L, Okamoto C, Hamm-Alvarez S (2011) A Rab11a-enriched subapical membrane compartment regulates a cytoskeleton-dependent transcytotic pathway in secretory epithelial cells of the lacrimal gland. *Journal of cell science* **124:** 3503-3514

Yang X, Zou J, Hyde DR, Davidson LA, Wei X (2009) Stepwise maturation of apicobasal polarity of the neuroepithelium is essential for vertebrate neurulation. *J Neurosci* **29:** 11426-11440

Yu W, Datta A, Leroy P, O'Brien LE, Mak G, Jou TS, Matlin KS, Mostov KE, Zegers MM (2005) Beta1-integrin orients epithelial polarity via Rac1 and laminin. *Mol Biol Cell* **16:** 433-445

Yu X, Prekeris R, Gould GW (2007) Role of endosomal Rab GTPases in cytokinesis. *Eur J Cell Biol* **86:** 25-35

Zhang L, Kendrick C, Julich D, Holley SA (2008) Cell cycle progression is required for zebrafish somite morphogenesis but not segmentation clock function. *Development* **135:** 2065-2070

Zigman M, Trinh le A, Fraser SE, Moens CB (2011) Zebrafish neural tube morphogenesis requires scribble-dependent oriented cell divisions. *Curr Biol* **21:** 79-86

Figure legends

Figure 1. Apical polarisation of cells at the tissue midline begins prior to the C-division

Dotted lines: midlines. Dashed lines: basal edges.

A. Time-lapse sequence showing a neural rod cell prior to, during and following C-division. Prior to division, the cell extends across the tissue centre and Pard3-GFP puncta broadly localise around the region where the cell intersects this point. Pard3-GFP puncta are biased to medial side of the cell at metaphase but subsequently are found at the cleavage plane between daughters (17/17 cells from 6 embryos) and later more precisely to the nascent apical surface (arrow). The first and last images are duplicated with the bright field shown in grey. The Pard3-GFP channel is shown separately and enlarged to the right. See also movie S1.

B. Dot plot showing distribution of midline crossing divisions from 3 embryos relative to their tissue midline (zero on Y-axis). Over time, the location of divisions near the midline becomes more precise.

C. Pard3-GFP puncta localise to the cleavage furrow in cells dividing very close to the midline (11/12 cells from 6 embryos).

D. Pard3-GFP puncta are biased to the medial side of cells that divide lateral to the midline (18/20 from 6 embryos). Pard3GFP then progressively localises to the cleavage plane between the two daughter cells.

Figure 2. Apical polarisation of cells at the tissue midline is independent of cell division

Dotted lines: midlines.

A. Division-blocked cells in *emi1*MO embryos frequently stretch completely across the width of the neural rod (36/84 from 5 *emi1*MO embryos, compared to 18/112 cells before C-division in 6 control embryos). Arrows indicate left and right sides of rod.

B to **D**. Time-lapse sequences of Pard3-GFP puncta localizing close to the region where division-blocked cells intersect the tissue midline. Pard3-GFP locates to the tissue midline irrespective of the length of the cells' contralateral process

(44/44 cells from 7 embryos: B=16 cells, C=10 cells, D= 18 cells). See also Movie S2.

E. Single Z-section demonstrates that puncta of ZO1 protein also appear at the region where division-blocked cells intersect the midline. The mGFP channel is shown separately with the outlines of individual example cells highlighted.

F. Time-lapse sequence of a division-blocked cell labelled with DCX-GFP. 23/23 cells from 5 embryos that extended beyond the tissue midline underwent microtubule reorganisation (arrow) close to the point at which the cell intersects the midline. 7 of these cells consequently retracted their contralateral microtubule bundles.

See also figure S1

Figure 3. A mirror-symmetric microtubule cytoskeleton is organised around the tissue midline

Dotted lines: midlines. Dashed lines: basal edges.

A. Timelapse sequence of centrosomal and nuclear movement within two cells from a wild-type embryo. The centrosomes (small arrows) from both cells gradually move towards the tissue midline. The initially lateral nuclei then relocate medially to the centrosomes, the centrosomes duplicate (arrowheads) and division occurs close to the midline (e.g. see nucleus from the lower cell, marked with an asterisk). The duplicated sister cells then extend towards the basal sides of the neural rod, locating their cleavage planes more precisely at the tissue midline and the centrosomes locate just laterally to each side of the midline (arrowheads). Of 24 cells from 5 embryos that extended across or near the tissue midline, 19 cells located their centrosomes close to the tissue midline and divided at this location. The division location of the 5 cells that divided more laterally was still coincident with the location of their centrosomes.

B. A division-blocked cell labelled with CENTRIN-GFP. 6/6 cells that extended beyond the tissue midline from 3 embryos localised their centrosomes close to the point at which they intersected the midline. Two spots of CENTRIN-GFP represent the duplicated centrosomes resulting from the *emi1*MO blocking M-phase entry.

C and D. EB3-GFP labelled cells showing plus-end directed growing microtubule comets.

Ci. A single z-plane of two division-blocked cells at a single timepoint.

Cii. A projection of 20 sequential time points from a single z-plane. Microtubule comets grew from MTOCs, located close to midline. Arrows mark the path taken by selected microtubule comets. 7/7 cells that extended across the middle of the tissue from 1 embryo had a mirror reversal of microtubule polarity close to the tissue centre (see also Movie S3).

Di. A z-projection of one wild-type cell at a single timepoint prior to division.

Dii. A projection of 29 sequential time points from a stack of 6 z-planes. A similar location of MTOCs close to the midline and a reversal of microtubule polarity around the tissue midline were seen in control cells prior to division. Arrows mark the path taken by selected microtubule comets. 14/14 cells from 6 embryos that extended across the middle of the tissue had a mirror reversal of microtubule polarity close to the tissue centre (see also Movie S4).

Diii. A timelapse sequence of the same cell as it carries out the C-division. After division, the MTOCs are gradually repositioned towards the midline. 14/14 pairs of cells from 7 embryos repositioned their MTOCs close to the midline.

Figure 4. Pard3 fusion proteins are mis-localised basally with nocodazole treatment

Dotted lines: midlines. Dashed lines: basal edges.

A. Dorsal view of DCX-GFP labelled NP cells within the hindbrain of a division-blocked embryo and treated with nocodazole from the 6-somite stage. After 10 minutes treatment the microtubule cytoskeleton is still in tact, with long DCX fibres present along the whole length of the cells. After 95 minutes the microtubules are depolymerised, resulting in disorganised and fragmented DCX fibres.

Bi. Low magnification dorsal view of right hand side of neural rod illustrating Pard3-RFP distribution in nocodazole treated embryo. Pard3-RFP appears at the basal end of cells (dashed line to right) after 105 minutes.

Bii. Pard3-GFP is lost from the apical pole (arrow) and distributes to the basal pole (arrowhead) of this cell within 75 minutes of the nocodazole treatment.

C. The percentage of cells expressing Pard3-FP only apically or not at all (blue) or at least partially basally (red) before and after nocodazole treatment. After nocodazole addition, 88% of cells contained some basal Pard3-FP, as opposed

to 12% of cells in control embryos (P<0.0001, Fisher's exact test). n=35 cells from 3 treated embryos and 28 cells from 3 control embryos.

Di. Recovery of apical Pard3-GFP (arrow) from basal (arrowhead) following nocodazole wash-out.

Dii. Recovery of apical Pard3-GFP from basal (arrowhead) following nocodazole wash-out. In this cell Pard3-GFP puncta were seen to decorate and travel along filamentous structures (arrows).

We monitored 16 out of 26 cells from 4 embryos that re-positioned Pard3-GFP from a basal to apical position following nocodazole wash out. The remaining cells either had an unclear morphology (n=3), delaminated from the epithelium (n=4) or died (n=3).

Figure 5. Pard3 and Rab11a are necessary for lumen formation

Dotted lines: midlines. Dashed lines: basal edges.

A, B. 3D reconstructions of dextran-filled brain ventricles from 28h.p.f. wild type (**A**) and Pard3-Δ6-EGFP (**B**) embryos. Ventricle morphology is severely disrupted in Pard3-Δ6-EGFP embryos.

C-H. A *Krox20-RFP-KalTA4* control embryo (**C-E**) and a *Krox20-RFP-KalTA4*x*UAS:mCherry-Rab11a-S25N* embryo (**F-H**) labelled with Pard3-GFP in horizontal orientation. A Z-projection of each embryo is shown at the 17-somite stage (**C, F)**, with the GFP channel shown separately (**D, G**). Pard3-GFP is able to localise to the apical midline in both embryos but intensity levels appear slightly lower in DNRab11a rhombomeres 3 and 5 (**F, G**). A montage of images for each embryo is shown 8 hours and 30 minutes later (26 h.p.f.), illustrating a single z-plane at the dorsal-most surface of the opening lumen (**E, H**). Whilst the lumen opens normally in control embryos (**E**), opening does not occur in Rab11aDN rhombomeres 3 and 5 in dominant negative embryos (**H**) (n=15/15 control embryos and 16/16 Rab11aDN embryos).

I. A projected stack of a division-blocked *Krox20-RFP-KalTA4*x*UAS:mCherry-R*ab11a-*S25N* 28-somite-stage embryo labelled with GFP-ZO1, H2B-RFP and CAAX-CHERRY in horizontal orientation. Disorganised lumen opening has started to occur in control rhombomeres 2, 4 and 6 but not in Rab11aDN rhombomeres 3 and 5.

J. Z-projection of mosaically labelled RAB11ADN-EGFP cells in a 22-somite stage neural rod. Pard3-RFP is localised normally to the apical end feet of the cells (e.g. arrow).

K-L. A projected stack of a *Krox20-RFP-KalTA4* 31 h.p.f. control embryo (**K**) and a *Krox20-RFP-KalTA4*x*UAS:mCherry-R*ab11a-*S25N* 31 h.p.f. embryo (**L**) labelled with ZO1 and sytox in horizontal orientation. White lines indicate the approximate position of the basal surfaces. A smooth lumen fully opens in control embryos (**K**), whilst in Rab11aDN embryos lumens lined by apical junctions were present in rhombomeres 2, 4 and 6 but no lumens were formed in rhombomeres 3 and 5 and junctional proteins were mislocalised (e.g. arrows) (**L**) (n=7/7 control embryos and 6/6 Rab11aDN embryos).

See also figure S2.

Figure 6. RAB11A traffics to the point where cells intersect the tissue midline and is mislocalised following nocodazole treatment

Brightfield images are shown in grey. Dotted lines: midlines. Dashed lines: basal edges.

A. Time-lapse sequence of a control cell expressing RAB11A-EGFP and dividing across the tissue midline. RAB11A-EGFP puncta broadly accumulate within a 15μm region close the tissue midline before C-division (n=15 cells from 4 embryos, standard error = 1.127μm. The nucleus then moves to this point and the cell divides across the midline. RAB11A-EGFP puncta then redistribute around the apical ends of the sister cells. See also Movie S5.

B. Time-lapse sequence of a division-blocked cell expressing RAB11A-EGFP. RAB11A-EGFP puncta are initially broadly distributed within an 18μm region near the midline (n= 13 cells from 2 embryos at 12 somites, standard error = 2.18μm). Puncta then progressively accumulate more precisely to a 6μm region near where the cell intersects the midline (n=9 cells from 2 embryos at 17 somites, standard error = 1.18μm). This accumulation coincided spatially and temporally with the appearance of the cell reorganisation near the nascent apical surface (arrow). See also Movie S6.

C. Division-blocked embryos were treated with nocodazole from early neural keel stages. The EGFP channel is shown separately. Before nocodazole treatment,

RAB11A-EGFP was broadly distributed around the tissue centre. RAB11A-EGFP was basally mis-localised following nocodazole treatment (arrowheads).

Figure 7. Cells integrate anti-basal signals with cell-cell interactions to determine localisation of apical complexes

Ai. Cartoon depicting physical separation of the two halves of the neural plate to delay convergence. Blue line is the plane of orientation for **Aii**.

Aii. A single horizontal z-plane of the hindbrain of a division-blocked embryo at the 18-somite stage in which convergence has been delayed. Cells were labelled with mGFP and H2B-RFP and subsequently stained for ZO1 immunoreactivity.. Where the left and right halves do not meet, ZO1 lines the superficial surface (arrowed) of the developing neuroepithelium. The superficial surface is seen *en face* on left hand side (arrowhead).

Aiii. Reconstruction in the transverse plane of left-right separated tissue (approximately at level of dotted line in Ai), showing ZO1 at the superficial tip of neural cell. Quantification showed 33/33 cells from 5 embryos localised ZO1 strongly at their most anti-basal tip, situated at the superficial surface.

B. Horizontally orientated hindbrain of a division-blocked embryo at the 8-somite stage, labelled with Ctnna-citrine. **(i)** A single z-plane showing that Ctnna-citrine accumulates along the cell membrane and is not restricted to the anti-basal extremity of the cell (n = 14 embryos). **(ii)** Cells on one side of the neural keel were mosaically labelled and the signal intensity increased to clearly show the cell outline. **(iii)** Cell morphologies (red) were mirrored (yellow) to create a predicted zone of interdigitation, overlying a z-projection of Ctnna-citrine. **(iv)** The zone of interdigitation is indicated by dashed lines and closely reflects the zone over which cells localise Ctnna puncta. Between 10 and 25 interdigitating cells were used to define the zone of interdigitation in each embryo (n = 8 embryos).

C. Horizontal 10μm z-projection of 15 somite stage embryo hindbrains injected with control or Laminin C1 morpholino and labelled with ZO1 and DAPI. Laminin C1 morphants had large areas of basally mislocalised ZO1, e.g. arrowheads (n=15), while control embryos never had basally located ZO1 (n=7).

Figure 8. Lumen surface is disrupted without division

A. Maximum z-projections of control and division-blocked embryos showing the hindbrain at 18h.p.f. and the spinal cord at 24 h.p.f. ZO1 immunoreactivity is shown separately in white and the otic vesicles are marked with asterisks. Control embryos had uninterrupted ZO1 along the midline. However, in division-blocked embryos the midline was interrupted by cell nuclei, resulting in gaps in ZO1 staining (arrows). This was found particularly prevalently but not exclusively at rhombomere boundaries.

B. Quantification of the number of gaps in ZO1 immunoreactivity at all dorsal-ventral levels in a 150μm region of each embryo adjacent to the otic vesicle. A two-tailed unpaired T-test was used. There were significantly more gaps in *emi1*-MO embryos (3.1) than control-MO embryos (0.86). $P<0.0001$. n=7 for both groups. Data are represented as a mean +/- S.E.M.

C. Maximum projections of dorsally oriented 22 and 24h.p.f. control and division-blocked embryos showed that lumen opening was disrupted and the lumen surface was ragged in division-blocked embryos. Lumen opening was particularly restricted at rhombomere boundaries (e.g. arrows).

D. Time-lapse sequence of a division-blocked cell showing the retraction of the contralateral process back to the shoulder region where the cell intersects the midline. This occurred in 58% (21/36) cells from 5 embryos. Bright-field is shown in grey. The tissue midline is indicated by a dotted line.

Figure 9. Graphical model of results

A. Summary of results for the role of interdigitation in polarisation. When division-blocked cells interdigitate normally (**i**), they localise apical proteins at the tissue midline at neural keel/rod stages. However, when interdigitation is prevented (**ii**), cells localise apical proteins to their most anti-basal extremity, coincident with the superficial surface. This suggests that the underlying apical polarisation of cells is anti-basal and that interdigitation is required to specifically localise this anti-basal polarisation around the point where cells intersect the tissue midline.

B. Summary of results for the role of the ECM in polarisation. When a normal ECM is present (**i**), apical proteins localise precisely to the tissue midline at neural rod stages. However, when ECM structure is disrupted (**ii**), apical proteins

are mislocalised basally. This suggests that the underlying anti-basal polarisation of NP cells is at least partly mediated by the ECM.

C. Model for a polarisation feedback loop. When cells interdigitate at the tissue midline at keel stages, we suggest that nascent adhesions are formed between contralateral cells (**i**). These could then recruit apical polarity protein puncta to the broad region of the midline (**ii**), which in turn could recruit centrosomes. Centrosomes could then organise a mirror-symmetric microtubule cytoskeleton, which would reinforce and refine the localisation of apical proteins to the midline (**iii**), allowing the formation of mature junctions.

D. Summary of results for the role of division and the microtubule cytoskeleton in polarisation. (**i**) In wild type embryos, cells undergo the C-division near the midline, efficiently redistributing sister cells on either side of the developing rod and localising apical proteins to the nascent lumen surface at their point of connection at the midline. This therefore allows normal lumen opening. (**ii**) When C-division is blocked, cells localise apical proteins to the tissue midline and some cells retract ectopic cell processes to the midline. However, this process is not efficient and many cells remain straddling the tissue midline. This therefore interrupts normal lumen opening. (**iii**) If microtubules are depolymerised in division-blocked cells using nocodazole, apical proteins localise ectopically at the basal surface. If microtubules are allowed to reploymerise by washing out nocodazole, apical proteins relocalise at the apical surface and lumen opening occurs.

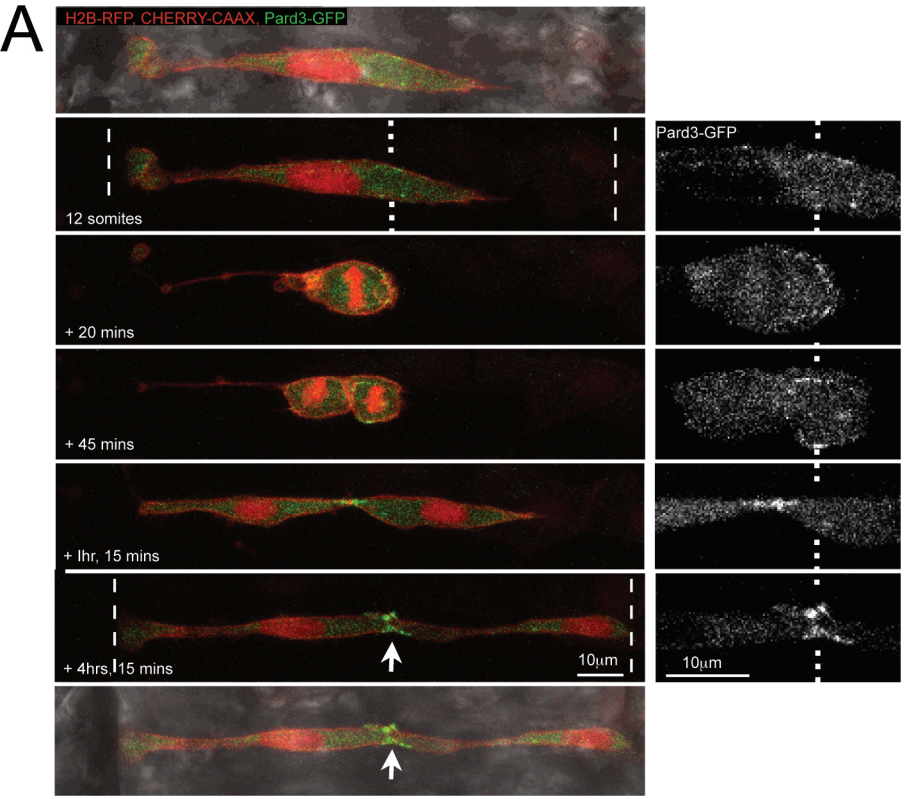
A
H2B-RFP, CHERRY-CAAX, Pard3-GFP
12 somites
+ 20 mins
+ 45 mins
+ 1hr, 15 mins
+ 4hrs,15 mins
10μm
Pard3-GFP
10μm

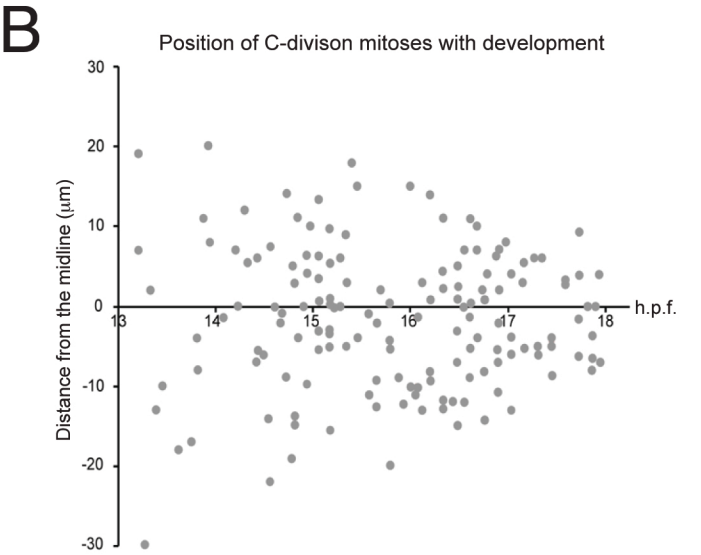
B
Position of C-divison mitoses with development
Distance from the midline (μm)
30
20
10
0
-10
-20
-30
13
14
15
16
17
18
h.p.f.

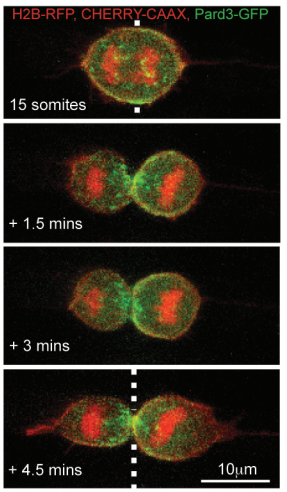
C
H2B-RFP, CHERRY-CAAX, Pard3-GFP
15 somites
+ 1.5 mins
+ 3 mins
+ 4.5 mins
10μm

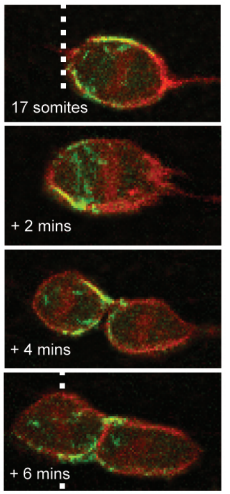
D
17 somites
+ 2 mins
+ 4 mins
+ 6 mins

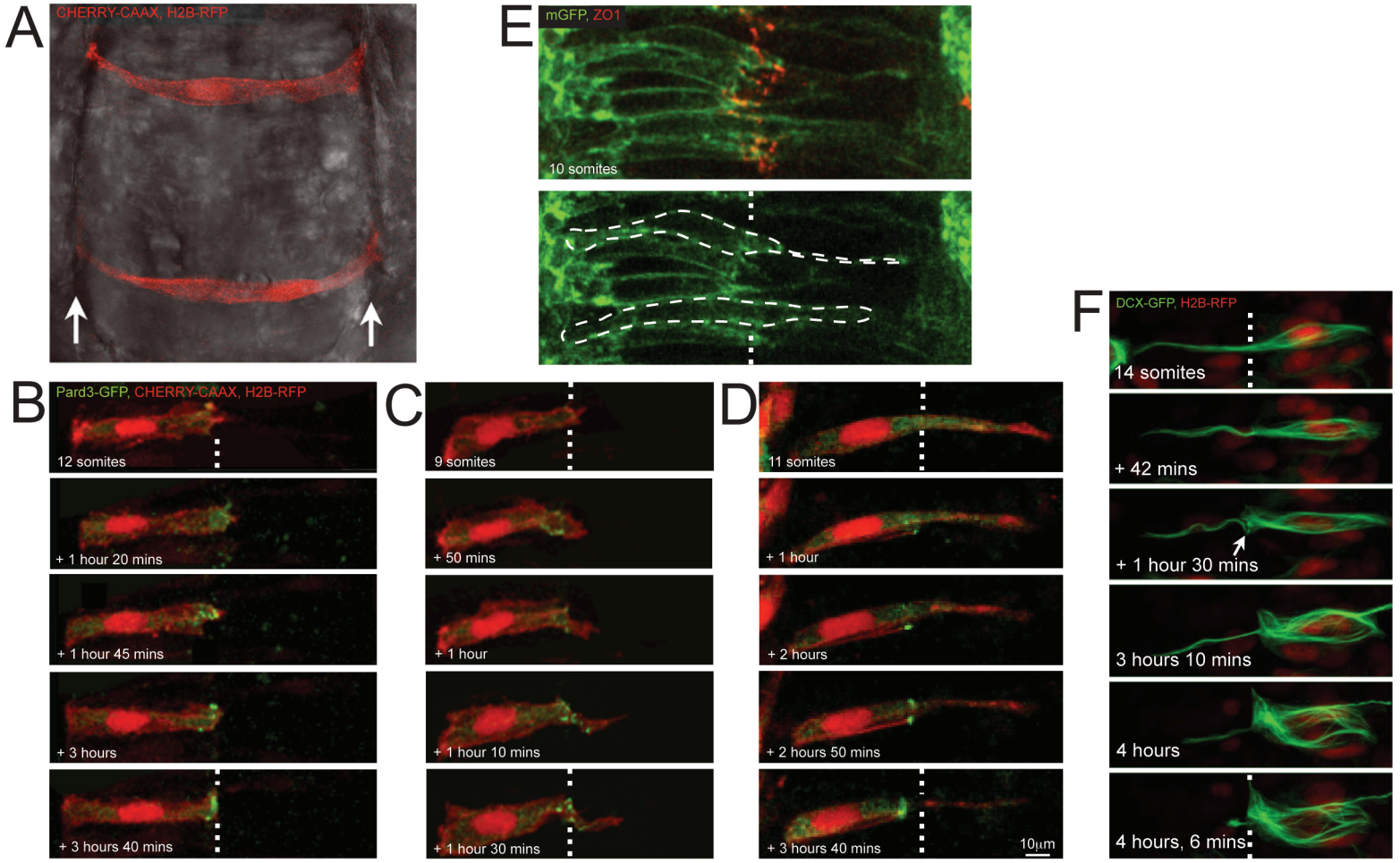
A
CHERRY-CAAX, H2B-RFP
E
mGFP, ZO1
10 somites
B
Pard3-GFP, CHERRY-CAAX, H2B-RFP
12 somites
+ 1 hour 20 mins
+ 1 hour 45 mins
+ 3 hours
+ 3 hours 40 mins
C
9 somites
+ 50 mins
+ 1 hour
+ 1 hour 10 mins
+ 1 hour 30 mins
D
11 somites
+ 1 hour
+ 2 hours
+ 2 hours 50 mins
+ 3 hours 40 mins
10μm
F
DCX-GFP, H2B-RFP
14 somites
+ 42 mins
+ 1 hour 30 mins
3 hours 10 mins
4 hours
4 hours, 6 mins

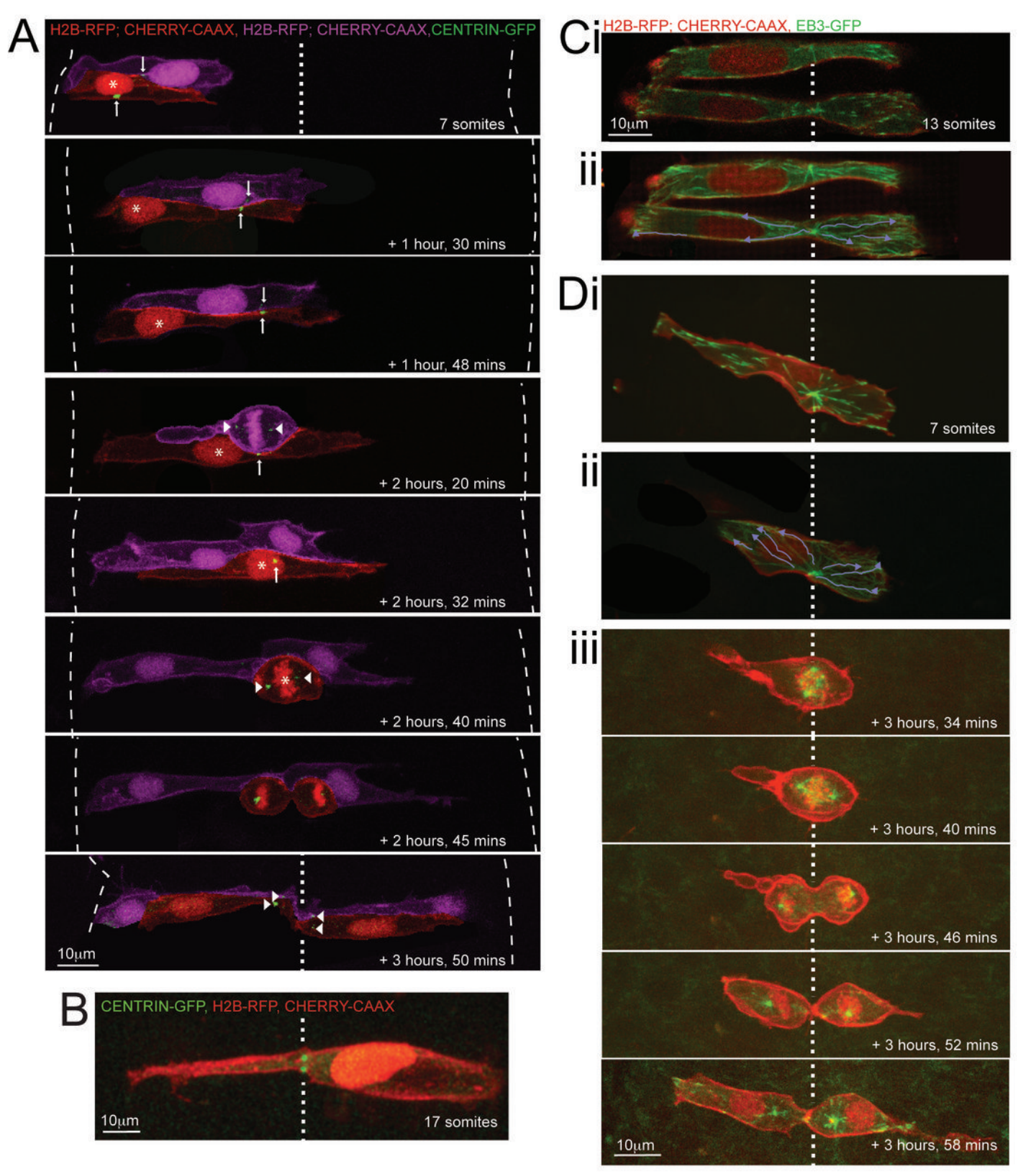
A
H2B-RFP; CHERRY-CAAX, H2B-RFP; CHERRY-CAAX,CENTRIN-GFP
7 somites
+ 1 hour, 30 mins
+ 1 hour, 48 mins
+ 2 hours, 20 mins
+ 2 hours, 32 mins
+ 2 hours, 40 mins
+ 2 hours, 45 mins
10μm
+ 3 hours, 50 mins
B
CENTRIN-GFP, H2B-RFP, CHERRY-CAAX
10μm
17 somites
Ci
H2B-RFP; CHERRY-CAAX, EB3-GFP
10μm
13 somites
ii
Di
7 somites
ii
iii
+ 3 hours, 34 mins
+ 3 hours, 40 mins
+ 3 hours, 46 mins
+ 3 hours, 52 mins
10μm
+ 3 hours, 58 mins

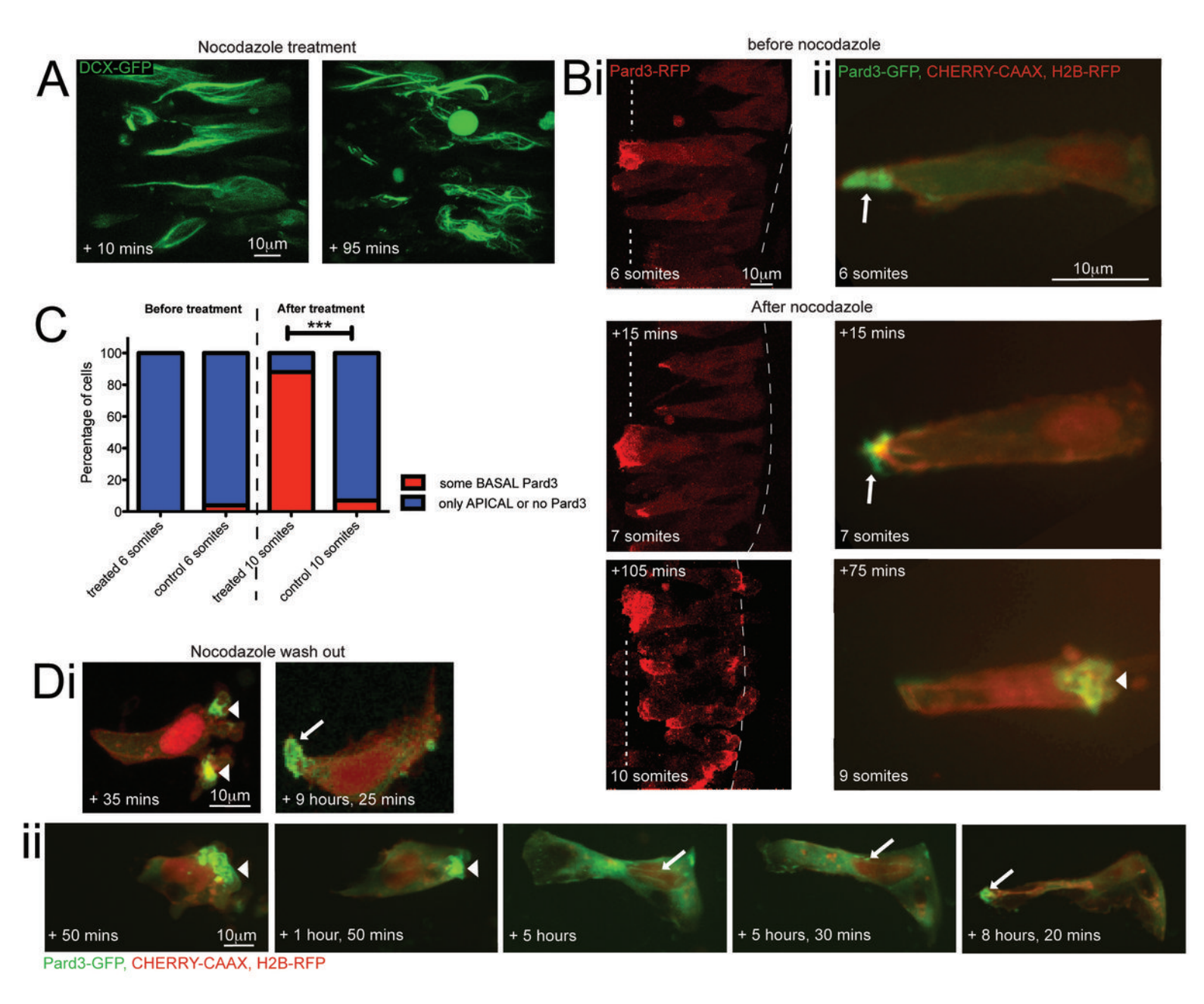
Nocodazole treatment
A
DCX-GFP
+ 10 mins
10μm
+ 95 mins
before nocodazole
Bi
Pard3-RFP
6 somites
10μm
ii
Pard3-GFP, CHERRY-CAAX, H2B-RFP
6 somites
10μm
C
Before treatment
After treatment
***
Percentage of cells
100
80
60
40
20
0
treated 6 somites
control 6 somites
treated 10 somites
control 10 somites
some BASAL Pard3
only APICAL or no Pard3
After nocodazole
+15 mins
7 somites
+15 mins
7 somites
+105 mins
10 somites
+75 mins
9 somites
Nocodazole wash out
Di
+ 35 mins
10μm
+ 9 hours, 25 mins
ii
+ 50 mins
10μm
+ 1 hour, 50 mins
+ 5 hours
+ 5 hours, 30 mins
+ 8 hours, 20 mins
Pard3-GFP, CHERRY-CAAX, H2B-RFP

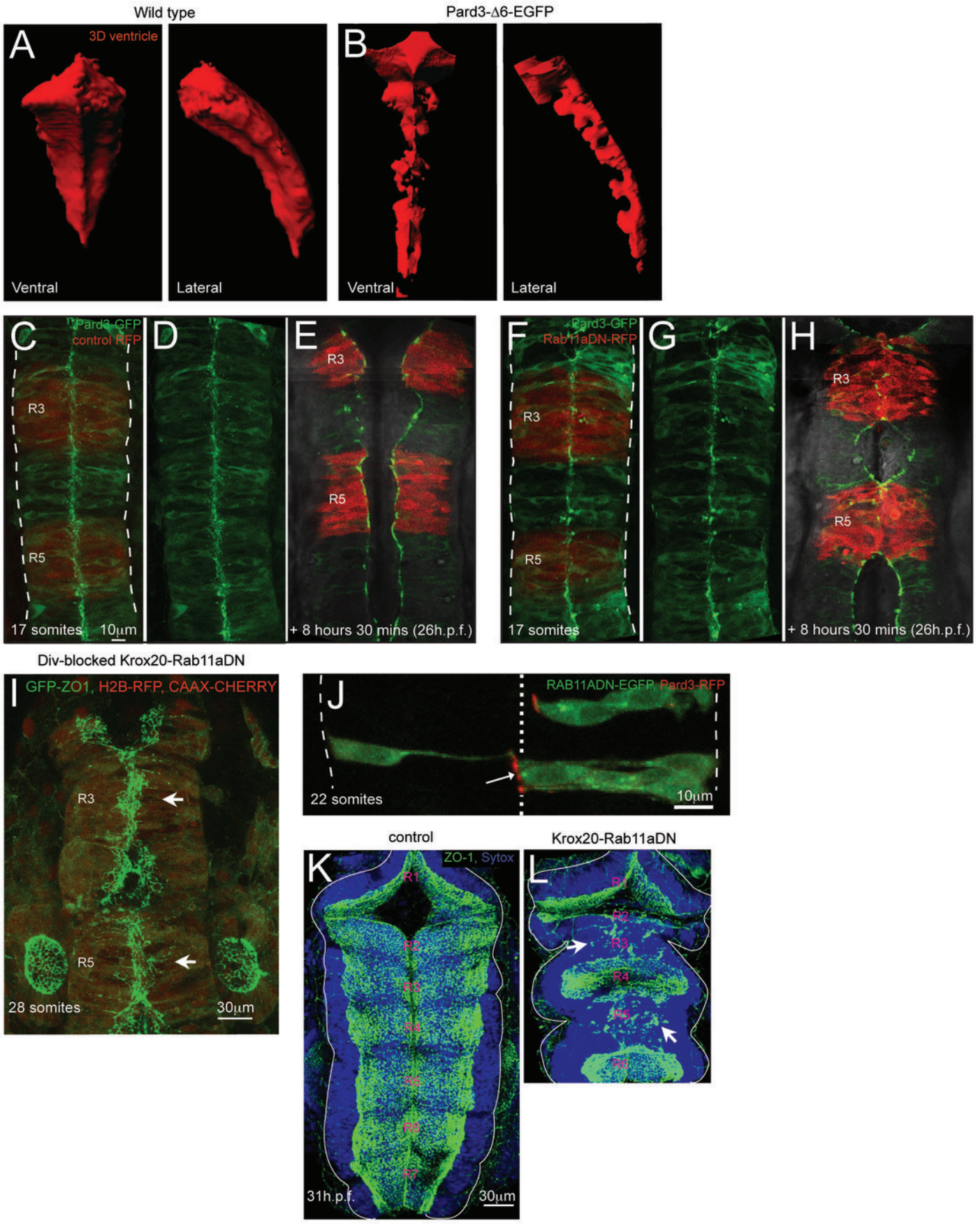
Wild type
Pard3-Δ6-EGFP
A
3D ventricle
Ventral
Lateral
B
Ventral
Lateral
C
Pard3-GFP
control RFP
R3
R5
17 somites
10μm
D
E
R3
R5
+ 8 hours 30 mins (26h.p.f.)
F
Pard3-GFP
Rab11aDN-RFP
R3
R5
17 somites
G
H
R3
R5
+ 8 hours 30 mins (26h.p.f.)
Div-blocked Krox20-Rab11aDN
I
GFP-ZO1, H2B-RFP, CAAX-CHERRY
R3
R5
28 somites
30μm
J
RAB11ADN-EGFP Pard3-RFP
22 somites
10μm
control
Krox20-Rab11aDN
K
ZO-1, Sytox
R1
R2
R3
R4
R5
R6
R7
31h.p.f.
30μm
L
R1
R2
R3
R4
R5
R6

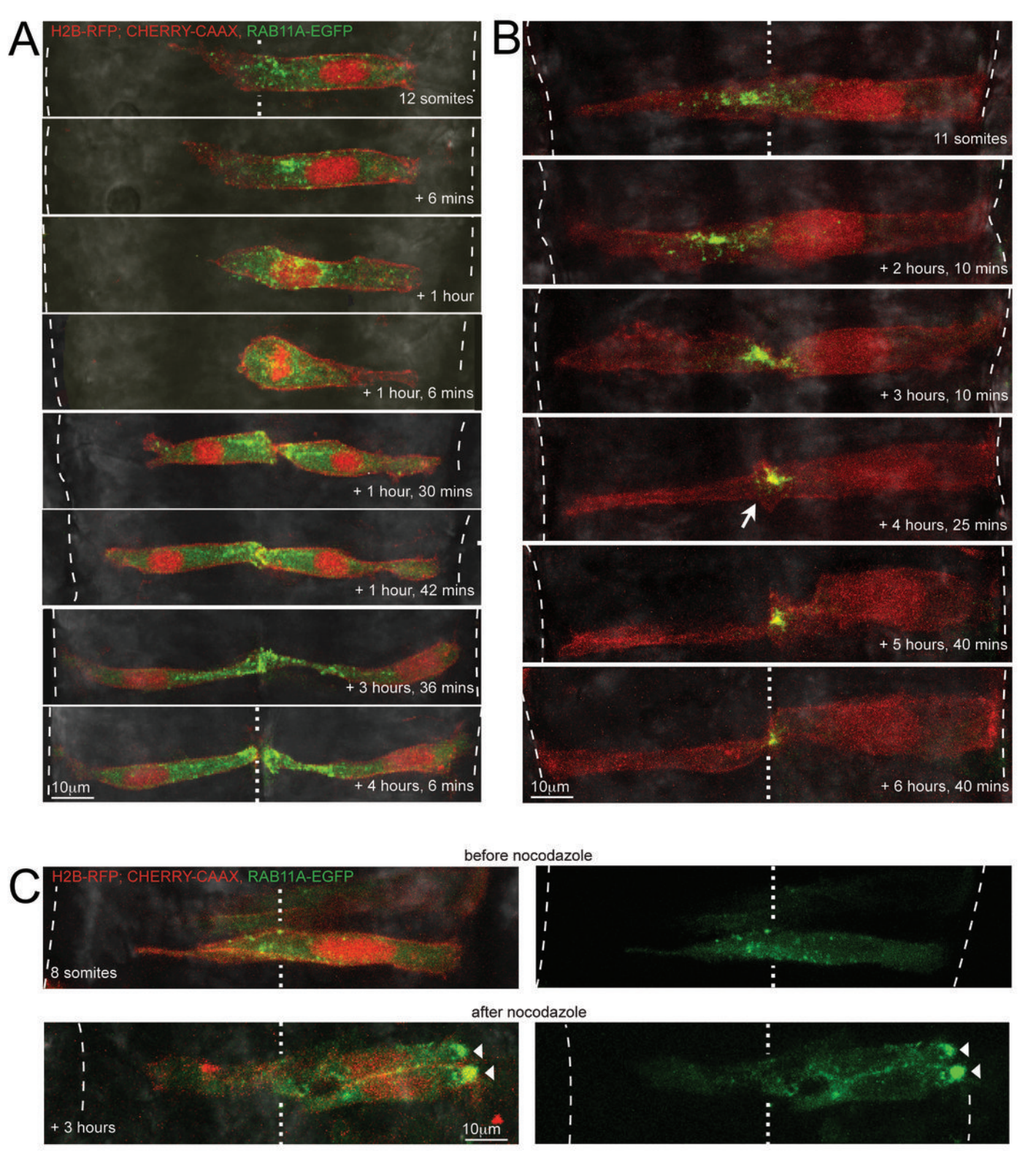
A
H2B-RFP; CHERRY-CAAX, RAB11A-EGFP
12 somites
+ 6 mins
+ 1 hour
+ 1 hour, 6 mins
+ 1 hour, 30 mins
+ 1 hour, 42 mins
+ 3 hours, 36 mins
+ 4 hours, 6 mins
10μm
B
11 somites
+ 2 hours, 10 mins
+ 3 hours, 10 mins
+ 4 hours, 25 mins
+ 5 hours, 40 mins
+ 6 hours, 40 mins
10μm
C
before nocodazole
H2B-RFP; CHERRY-CAAX, RAB11A-EGFP
8 somites
after nocodazole
+ 3 hours
10μm

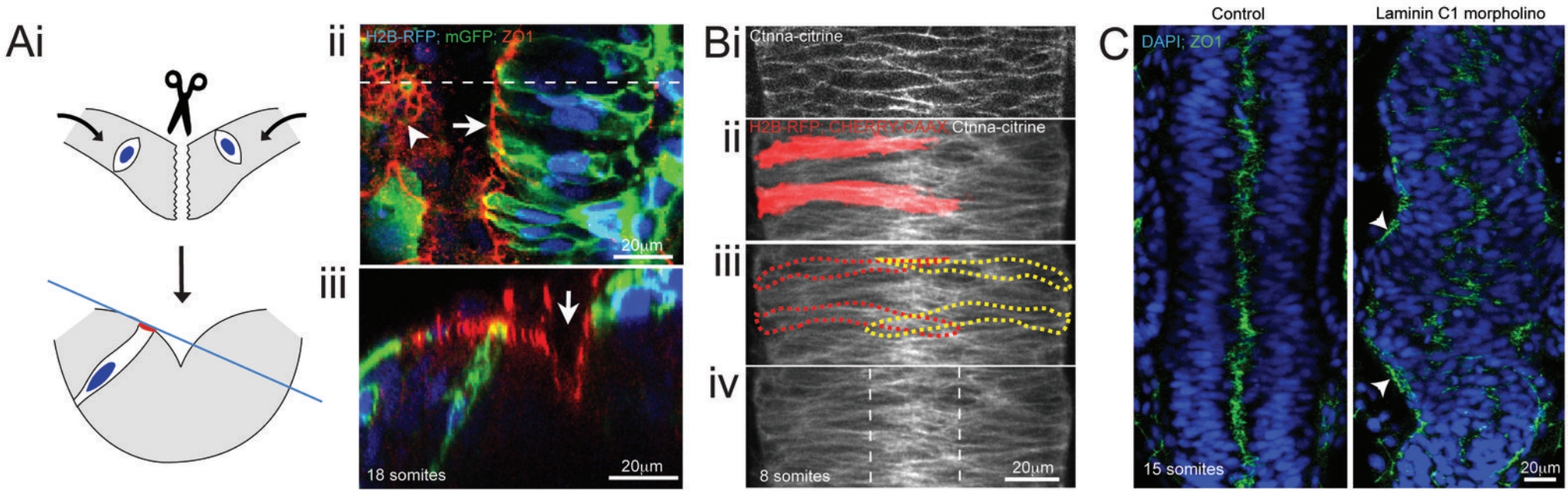
Ai
ii
H2B-RFP; mGFP; ZO1
20μm
iii
18 somites
20μm
Bi
Ctnna-citrine
ii
H2B-RFP; CHERRY-CAAX; Ctnna-citrine
iii
iv
8 somites
20μm
C
Control
Laminin C1 morpholino
DAPI; ZO1
15 somites
20μm

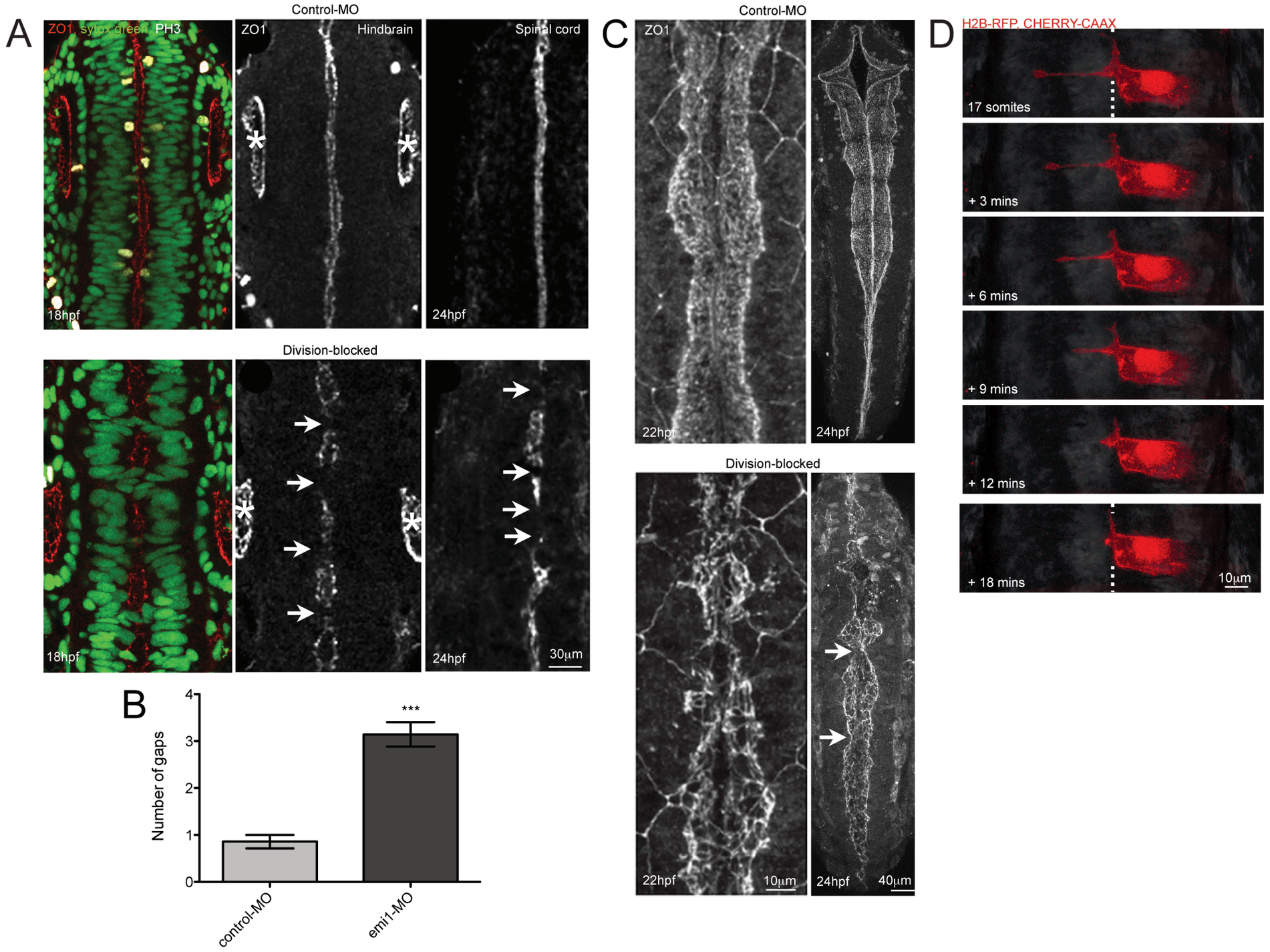
A
Control-MO
ZO1, sytox green, PH3
ZO1
Hindbrain
Spinal cord
18hpf
24hpf
Division-blocked
18hpf
24hpf
30μm
B
Number of gaps
***
control-MO
emi1-MO
C
Control-MO
ZO1
22hpf
24hpf
Division-blocked
22hpf
10μm
24hpf
40μm
D
H2B-RFP, CHERRY-CAAX
17 somites
+ 3 mins
+ 6 mins
+ 9 mins
+ 12 mins
+ 18 mins
10μm

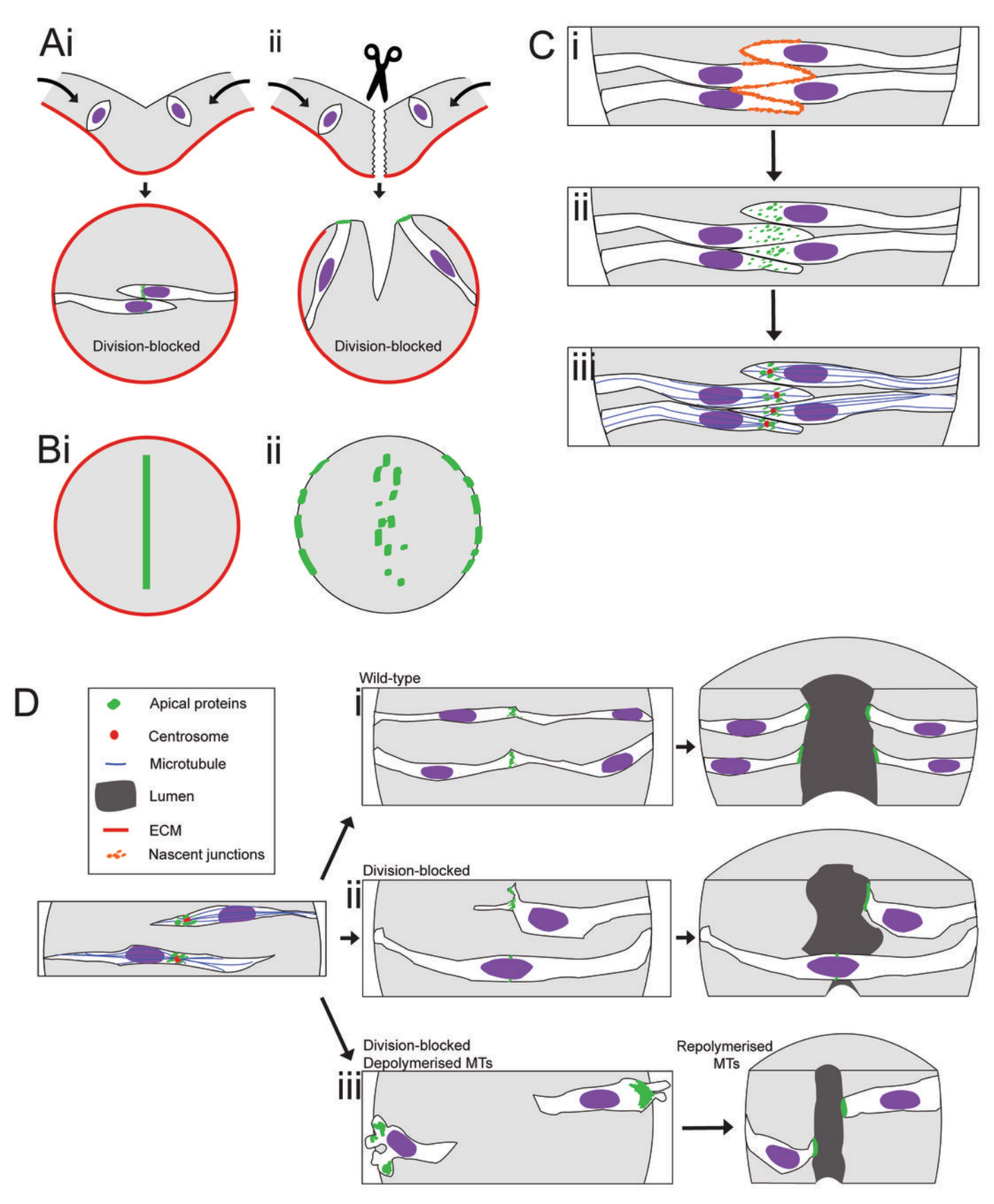
Ai
ii
Division-blocked
Division-blocked
C
i
ii
iii
Bi
ii
D
Apical proteins
Centrosome
Microtubule
Lumen
ECM
Nascent junctions
Wild-type
i
Division-blocked
ii
Division-blocked
Depolymerised MTs
iii
Repolymerised
MTs